Journal of Photochemistry and Photobiology A: Chemistry 222 (2011) 323–329

Contents lists available at ScienceDirect

Journal of Photochemistry and Photobiology A: Chemistry

journal homepage: www.elsevier.com/locate/jphotochem

Study of photocatalytic damages induced on *E. coli* by different photocatalytic supports (various types and TiO_2 configurations)

Marie Faure[a,b], Fabien Gerardin[b], Jean-Claude André[a], Marie-Noëlle Pons[a,*], Orfan Zahraa[a]

[a] *Laboratoire Réactions et Génie des Procédés, UPR 3349 CNRS, 1 rue Grandville BP20451, 54001 Nancy Cedex, France*
[b] *Institut National de Recherche et de Sécurité, Rue du Morvan, CS60027, 54519 Vandoeuvre Cedex, France*

ARTICLE INFO

Article history:
Received 21 March 2011
Received in revised form 26 June 2011
Accepted 2 July 2011
Available online 12 July 2011

Keywords:
Photocatalytic degradation
E. coli
Antibacterial
Metabolic damage
Monte Carlo approach

ABSTRACT

Photocatalysis, based on UV irradiation of a TiO_2 support to generate oxygen free radicals, has been shown to have antibacterial properties, but the process has yet to be optimized. Photocatalytic inactivation of Gram negative bacteria, *E. coli*, was studied on five different photocatalytic supports, in terms of TiO_2 type (Degussa P25/Millennium PC500) and configurations (catalyst was impregnated on supports, alone or with binder, or suspended in water). Several irradiation times were tested. Effective UV-A doses were estimated using a simulation based on a Monte Carlo approach to facilitate comparison between supports. For the same TiO_2 type, inactivation efficiency was best with the "suspension" configuration (up to 4 log in 120 min) followed by the "impregnated without binder" configuration (up to 2 log in 120 min) and finally the configuration with binder (only 0.5 log after 120 min). In the "suspension" configuration, TiO_2 P25 appeared to be more effective than TiO_2 PC500. This may be due to smaller dispersed particle sizes. Our experiments highlight the importance of optimizing contact between the bacteria to be inactivated and titanium dioxide particles. Bacterial regrowth was compared on two culture media with different nutrients, and revealed metabolic damage induced by photocatalysis. Based on the classical Chick–Watson model, the kinetics of the photocatalytic process were determined, including a lag time for several supports.

1. Introduction

Microorganisms are commonly inactivated by ionization [1–3], ozonation [4], germicidal UV-C [5–9] or in solution by chemical disinfection such as chlorination for example. Photocatalysis was initially used to eliminate pollutants in water [10,11] or air [12,13] purification. It has recently been shown to have antiviral [14], antifungal [15] and particularly potent antibacterial [16,17] properties. The photocatalytic process generally involves the use of UV radiation combined with a semi-conductor, most frequently titanium dioxide, present as a photocatalytic nano-powder. Excitation of TiO_2 by UV-A forms an electron-hole pair which generates $OH^\bullet$ and $HO_2^\bullet$ free radicals by contributing to the H_2O and O_2 redox reaction. Hydroxyl radical is highly reactive and leads to strong oxidation of pollutants adsorbed on the catalyst's surface, resulting in complete mineralization for many compounds.

Most experiments showing the bactericidal effect of photocatalysis were performed in aqueous solution [18–21]. Airborne experiments (i.e. photocatalytic degradation of microorganisms dispersed into the air) are rare because generating of a homogeneous, stable bio-aerosol remains difficult and the experimental setup is complex [22]. Because of this, some authors have used a batch approach, where bacteria (suspended in water for example) are spread on photocatalytic supports. This approach has been used to study the influence of parameters such as irradiation [23,24], nature and quantity of TiO_2 [17–25] or duration of exposure [17,23,26]. Many of these tests used the model bacterium *E. coli*.

The main aim of the present contribution is the knowledge improvement of the antibacterial photocatalytic action by identifying the type of cell damage through comparison of bacterial growth on two culture media after exposure to the photocatalytic process. These tests are easily realized and aim at underline cell damage. Obviously they could be completed by more specified experiments. A batch approach was applied to compare several photocatalytic supports and revealed the importance of the nature and duration of contact between the bacterial cells and titanium dioxide. Photocatalytic inactivation tests on *E. coli* were conducted on 5 different supports. One of these was commercially available and the others were made in the laboratory. We chose TiO_2 configuration as a variable criterion to investigate the importance of the contact between bacterial cells and semiconductor for inactivation efficiency.

Furthermore, a kinetic analysis of bacterial inactivation by photocatalysis based on empirical methods such as Chick–Watson model [27] is performed in this study. Finally, some information

* Corresponding author. Tel.: +33 383175277.
E-mail address: Marie-Noelle.Pons@ensic.inpl-nancy.fr (M.-N. Pons).

1010-6030/$ – see front matter © 2011 Elsevier B.V. All rights reserved.
doi:10.1016/j.jphotochem.2011.07.003

are proposed to simulate light scattering in photocatalytic reactors and to assess the proportion of photons emitted by the lamp really available for the photocatalytic reaction with a Monte Carlo approach [28].

2. Materials and methods

2.1. Bacterial culture preparation and analysis

An *E. coli* strain from the Institut Pasteur collection (CIP 53.126) was subcultured on a Petri dish containing Tryptic Soy Agar medium (TSA, AES Chemunex, Bruez, France) for 24 h at 37 °C. Cells recovered from this dish were transferred into sterile Tryptone-Salt solution (TS, AES Chemunex) and grown to an optical density of 0.5 at 600 nm. 2 mL of this preparation were added to 25 mL of Lactose Broth (LB, AES Chemunex) before incubation for 24 h at 37 °C on a rotary shaker at 100 rpm. Cells were harvested by centrifugation at 7000 × *g* for 7 min and washed three times with sterile water. The concentration of the bacterial culture was determined on 10-fold serial dilutions in tryptic salt solution. A 0.1 mL sample of three successive dilutions was spread on two nutrient agar medium plates and incubated at 37 °C for 24 h. Colonies were counted on plates with between 15 and 300 colonies. The number of colony forming units present in the sample (N in CFU mL^{-1}) was estimated for two successive dilutions using relation (1) [29]:

$$N = \frac{\sum C}{v(n_1 + 0.1n_2)d} \quad (1)$$

where $\sum C$ is the number of colonies counted on all plates, v is the volume spread on plates, n_1 the number of plates considered for the first dilution, n_2 those considered for the second dilution and d is the dilution factor for the first dilution.

In line with French norms [30], a 95% confidence interval (Δ) was calculated for the number of colony forming units using Eq. (2).

$$\Delta = \frac{\sum C}{B} + \frac{1.92}{B} \pm \frac{1.96\sum C}{B}\frac{1}{d} \quad \text{with } B = v(n_1 + 0.1n_2) \quad (2)$$

For experiments, the bacterial culture was diluted 50-fold to obtain a concentration between 1.0×10^7 CFU mL^{-1} and 1.3×10^7 CFU mL^{-1}.

2.2. Photocatalytic supports

Photocatalytic tests were performed using 5 different single-use supports:

(1) Commercial support (Ahlstrom, Pont Evêque, France) composed of cellulose fibers, uncoated (reference 1045). Samples (4 cm^2) were autoclaved for 15 min at 121 °C to sterilize them before performing tests;
(2) Commercial support (Ahlstrom, Pont Evêque, France) coated with a mixture of TiO_2 PC500 Millennium (18 g m^{-2}) (Millennium Inorganic Chemicals, Thann, France), zeoliths (2 g m^{-2}), and SiO_2 (20 g m^{-2}) (reference 1048). Samples (4 cm^2) were autoclaved for 15 min at 121 °C to sterilize them before performing tests.
(3) Quartz media filters, (QMA, Whatman, Kent, UK) (25 mm in diameter) used alone without TiO_2 and sterilized by heating to 250 °C for 2 h.
(4) Quartz media filters, (QMA, Whatman, Kent, UK) (25 mm in diameter) impregnated with (P25 Degussa (2.2 g m^{-2}) (Evonik Degussa Corporation, Essen, Germany) or PC500 Millennium (1.8 g m^{-2})). For impregnation, either filters were immersed in P25 TiO_2 (4 g L^{-1} in water) for 10 s, or they were spread with a suspension of PC500 TiO_2 (4 g L^{-1} in water). Filters were then dried. QMA filters were sterilized by heating to 250 °C for 2 h.
(5) "Suspension" configuration, TiO_2 was dispersed in sterile water (1 g L^{-1}). The solution was then autoclaved (15 min, 121 °C). Bacteria were mixed with the TiO_2 suspension and the mixture was spread on previously sterilized blank QMA filters.

Table 1
TiO_2 characteristics [40].

Composition	Degussa P25 80% anatase–20% rutile	Millennium PC500 100% anatase
Particle size (crystallites) (nm)	30	10–15
Dispersed particle size (nm)	200–215	600–700

All supports were placed on glass slides to facilitate handling. Microscopic observations of some supports are shown in Fig. 1, and TiO_2 characteristics are listed in Table 1.

2.3. Photocatalytic reactor and light flux

Photocatalytic inactivation tests were performed in a reactor composed of a stainless steel cylinder (0.80 m in length and 0.20 m in diameter) fitted with a UV-A lamp (BLB, Philips TLD 18 W) (see Fig. 2) with an emission peak centered on 365 nm and a light intensity of about 1.1×10^{-5} Einstein s^{-1} (E s^{-1}). The chamber allowed simultaneous exposure of 6 photocatalytic supports placed 0.11 m from the lamp.

The titanium dioxide on the different photocatalytic supports only absorbed some of the light flux. Experimental measurement of the quantity of photons effectively available for bacterial inactivation was difficult. Therefore, we simulated the light trajectories in the chamber using a Monte Carlo approach [31,32]. This method is based on a statistically significant number of photons emitted by the lamp. For each emitted photon, a random number sequence is initiated that locates its position on the light source and its three directions of space (Φ,θ,z) in the reactor. The fate of each photon is followed until it is either absorbed at the catalyst surface or is lost on the surroundings. If the photon does not hit the catalyst surface, it is discarded and assumed to be lost, and the process is started again. At the end of the test, the flow of absorbed photons by the catalyst is determined. The principle of the simulation is presented in Fig. 3 (i_{max} = 30,000 photons).

To optimize modeling, the optical properties of both stainless steel and the photocatalytic supports (in terms of absorption, transmission and reflection) were experimentally determined for wavelengths between 300 and 400 nm using a UV/Vis/NIR spectroradiometer (Lambda 950, PerkinElmer, Courtaboeuf, France). Experiments were performed on wet supports with and without TiO_2 to determine the proportion of photons effectively absorbed by the photocatalyst.

2.4. Experimental procedure

Before conducting inactivation tests, each sterilized photocatalytic support was humidified with 0.15 mL sterile water. An aliquot of bacterial culture (0.10 mL) was deposited onto wet supports, before UV-A irradiation. Samples were harvested from the supports in 19.90 mL sterile water after irradiation. An aliquot of harvested cells (1 mL) was serially diluted 10-fold in tryptic salt solution. An aliquot of diluted solution (0.1 mL) was spread on nutrient agar medium plates. The number of colony forming units was determined after incubation at 37 °C for 24 h.

Growth was compared on two growth media: Tryptic Soy Agar, or complete medium (15 g L^{-1} pancreatic digest of casein, 5 g L^{-1} papaic digest of soya bean, 5 g L^{-1} sodium chloride, 15 g L^{-1} agar);

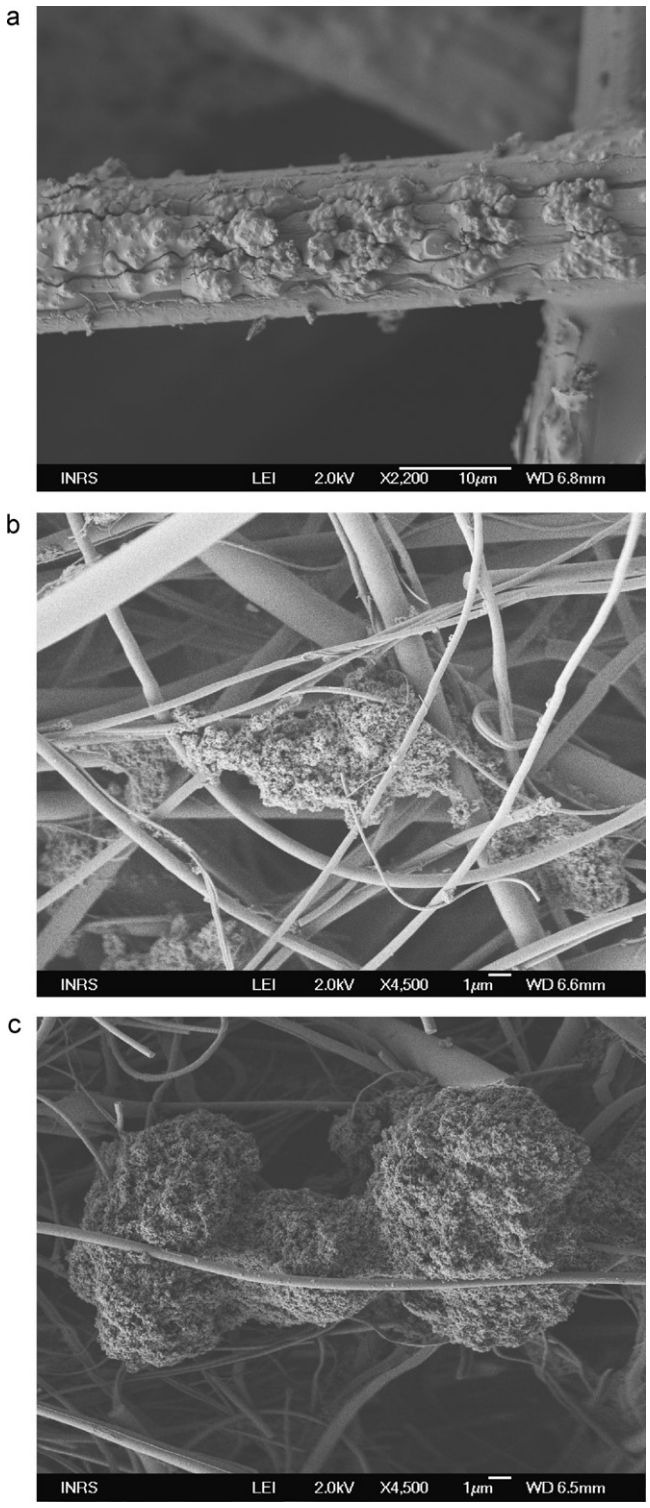

Fig. 1. SEM observations of photocatalytic supports (a) commercial photocatalyst, (b) P25 impregnated QMA, and (c) suspended P25 on QMA.

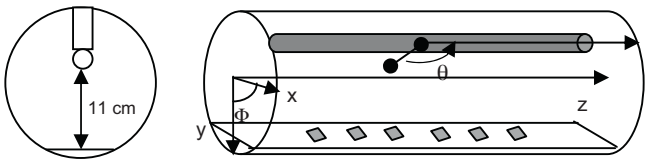

Fig. 2. Photocatalytic reactor.

or Eosin Methylene Blue (EMB, AES Chemunex) (10 g L^{-1} pancreatic digest of gelatin, 10 g L^{-1} lactose, 2 g L^{-1} dipotassium phosphate, 0.065 g L^{-1} methylene blue, 0.40 g L^{-1} eosine Y, 15 g L^{-1} agar). Any differences between the numbers of colony forming units counted on these two growth media after the photocatalytic process may be indicative of metabolic damage. According to Ray and Speck [33], changes in overall metabolic activity can be determined based on the growth response of stressed bacteria. This can be used to assess the cumulative effect of several structural and functional changes [33,34].

To determine the effect of photocatalysis, four experimental conditions were tested: with TiO_2/with UV-A (photocatalysis); with TiO_2/without UV-A (adsorption–adhesion); without TiO_2/with UV-A (photolysis); without TiO_2/without UV-A (control). The efficiency of photocatalytic inactivation was assessed over four irradiation times (20, 40, 60 and 120 min). The duration of exposure was extended for one support to highlight its maximal capacities. Each experiment was performed in triplicate, thus there were twelve bacterial samples for each irradiation time.

2.5. Photocatalytic inactivation efficiency

The experimental photocatalytic inactivation efficiency (E) was determined using Eq. (3):

$$E = \frac{N_0 - N_{\text{with } TiO_2/\text{with UVA}}}{N_0} \times 100 \quad (3)$$

where N is the number of CFU in the harvested suspension and N_0 the number of CFU in the bacterial culture deposited onto the support. We used the criteria established by Sayilkan et al. [35] to rank reduced bacterial cultivability: less than 20% reduction indicates no bactericidal effect; between 20% and 50% reduction signifies a low bactericidal effect; between 50% and 70% reduction corresponds to a moderate bactericidal effect; greater than 70% reduction was considered a significant bactericidal effect.

2.6. Kinetic model

The kinetics of photocatalytic bacterial inactivation are usually described using empirical equations. The Chick–Watson equation is the classical model for microorganism inactivation with a constant concentration of disinfecting agent [27], as expressed by Eq. (4):

$$\log\left(\frac{N}{N_0}\right) = -kt \quad (4)$$

where N/N_0 is the reduction in bacterial concentration, k is the kinetic constant of inactivation and t is time.

A lag phase is often noted at the beginning of the reaction. In this case, the delayed Chick–Watson model, which includes a second parameter (t_0) corresponding to the lag time, should fit the experimental results better (Eq. (5)).

$$\log\left(\frac{N}{N_0}\right) = \begin{cases} 0 & \text{for } t \le t_0 \\ -k(t - t_0) & \text{for } t \ge t_0 \end{cases} \quad (5)$$

Comparison of supports with different TiO_2 loads was based on Eq. (6):

$$\frac{1}{m_{TiO_2}} \log\left(\frac{N}{N_0}\right) = \begin{cases} 0 \text{ for } t \le t_0 \\ -k''(t - t_0) \text{ for } t \ge t_0 \end{cases} \quad \text{where } k'' = \frac{k}{m_{TiO_2}} \quad (6)$$

3. Results and discussion

3.1. Testing configurations

For each photocatalytic support the impact of photocatalysis on *E. coli* viability and cultivability was determined using four

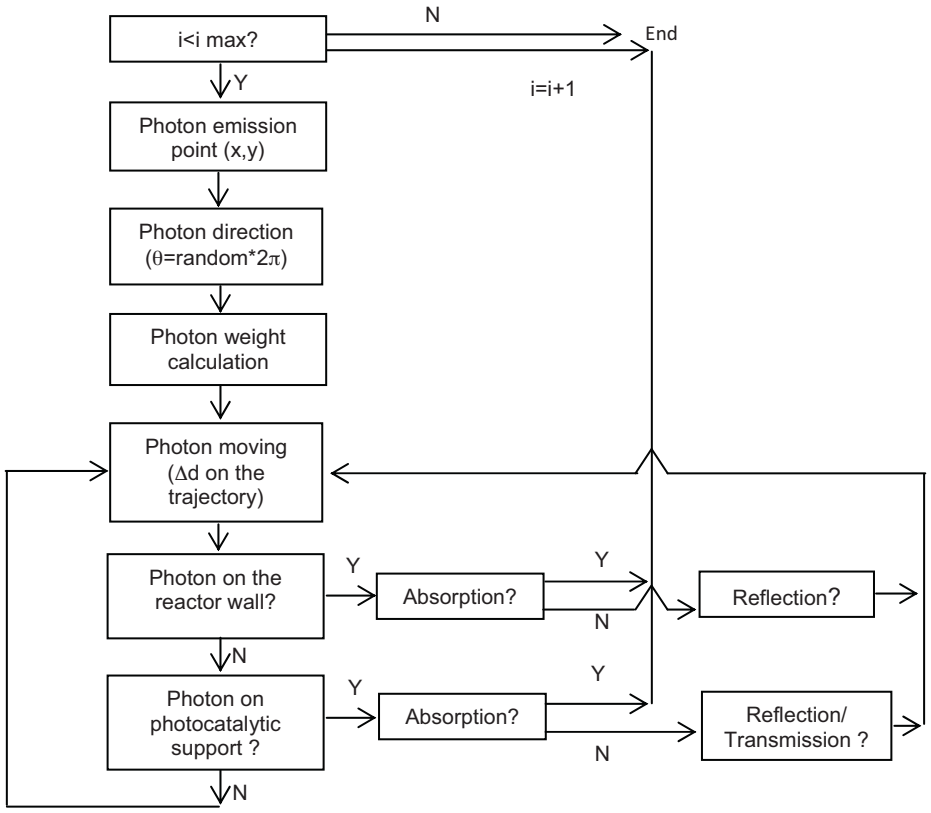

Fig. 3. Monte Carlo algorithm for simulation of light trajectories in the photocatalysis chamber and on phototcatalysis supports.

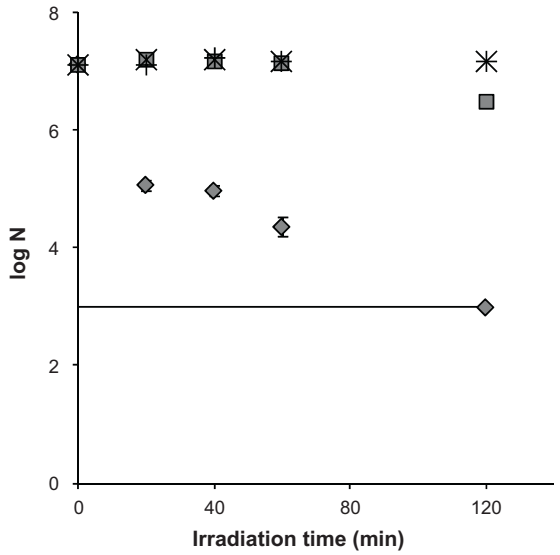

Fig. 4. Concentration of *E. coli* on QMA + TiO_2 P25 suspended; growth medium: TSA (— detection limit, ■ with UV-A/without TiO_2, ◆ with UV-A/with TiO_2, × without UV-A/without TiO_2, + without UV-A/with TiO_2).

configurations. The term "viability" defines the living character of the bacterium and "cultivability" its ability to develop and form colonies. A bacterium can be viable but not cultivable when it is stressed for example. The extent of *E. coli* inactivation for different irradiation times on P25-impregnated QMA filter is shown in Fig. 4.

The control sample (without TiO_2/without UV-A) concentration was the same as the initial concentration, indicating that cell harvesting from the supports was effective and that loading, experimentation and harvesting do not affect bacterial viability or cultivability, even after several hours in ultrapure sterile water. Ultrapure sterile water was used for all experiments.

An effect of the "with TiO_2/without UV-A" configuration could be interpreted as an adsorption/adhesion effect and/or as a direct bactericidal effect of titanium dioxide. Indeed, Liu et al. [36] recently showed that fresh TiO_2 could inactivate bacteria without UV-A excitation. In our experiments, however, no effect of TiO_2 was observed in the absence of irradiation (Fig. 4). *E. coli* can be inactivated by UV-A alone if irradiation time is sufficient (120 minutes) [37] and if the support has appropriate optical properties, such as those of quartz (blank QMA). In contrast with blank QMA, no effect was observed for the blank Ahlstrom support at 120 min. Measurement of the light absorption coefficients for the various supports without TiO_2 showed differences. Results for blank QMA and for 1045-Ahlstrom support, for wavelengths ranging from 300 to 400 nm, are shown in Fig. 5. Globally, the light absorption coefficient is higher for 1045-Ahlstrom than for blank QMA. Thus, when irradiated by the same quantity of photons, more photons are absorbed in 1045-Ahlstrom support than blank QMA and in this case, less photons are available for direct bacterial inactivation by light. The quartz material allows a better light transmission into the support where are bacteria than cellulose fibers.

To conclude this part and towards the different configurations, these results indicate that a photocatalytic effect is likely to be responsible for the loss of bacterial viability–cultivability observed for the "with UV-A/with TiO_2" condition shown in Fig. 4.

3.2. Light flux

Simulations indicated the number of photons emitted from the lamp and absorbed by TiO_2. Given the light flux generated by the lamp (1.1×10^{-5} E s^{-1}) it is possible to calculate the flux exciting the catalyst. Only 0.1% of photons ($\approx 10^{-8}$ E s^{-1}) were found to be absorbed by titanium dioxide on the five photocatalytic supports

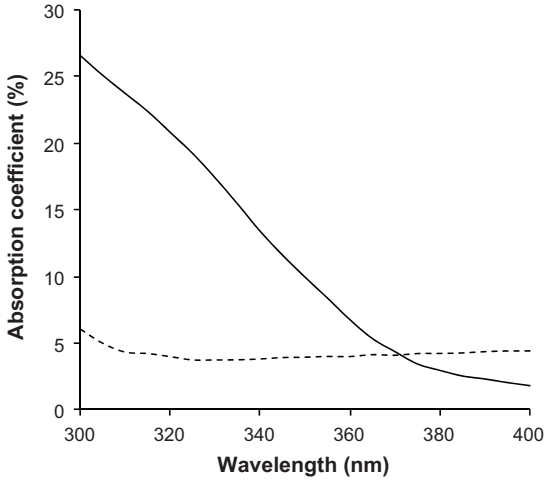

Fig. 5. Light absorption coefficient for supports without titanium dioxide (— Ahlstrom 1045, - - - - blank QMA).

(Table 2). The small differences observed between the different supports could be due to uncertainties linked to both experimental and simulated data (TiO_2 distribution on supports, particle size, random function used in the algorithm, etc.).

These data were used to estimate the UV-A dose exciting TiO_2 after 20–40–60 or 120 min of irradiation. Thus, photocatalytic supports could be compared for an equivalent UV-A dose by plotting graphs as a function of quantity of photons absorbed by TiO_2 rather than time.

3.3. Photocatalytic inactivation of bacteria

3.3.1. Irradiation time and metabolic effects

Inactivation of *E. coli* depends on irradiation time for all supports (Table 3). As described in the literature, better inactivation is achieved with longer irradiation times due to the production of more hydroxyl radicals, causing more damage to bacteria [38]. Both growth media (EMB and TSA) show similar results for this effect. At initial time the number of colony forming units counted on both media were the same for all samples. However, for the same sample and after photocatalytic process, the number of CFU counted on EMB was always lower than on TSA, indicating that that bacteria were not able to use (in the same way) nutrients present in EMB after photocatalytic process: they are metabolically damage. As EMB contains lactose (comparing with TSA which does not contain it) we supposed that lactose metabolism was affected during the photocatalytic process (see Table 3) [33]. Depending on the photocatalytic support used, different degrees of inactivation of this pathway were observed. Supports can be ranked in ascending order of efficacy: Ahlstrom, PC500 impregnated, P25 impregnated, PC500 suspended, P25 suspended. These differences can be explained by the TiO_2 type (P25, PC500) or how it was loaded onto the filter (impregnated with or without binder, suspended). For all supports, the photocatalytic process requires long irradiation times (several minutes to several hours) to induce significant loss of bacterial viability.

Table 2
Photons available for photocatalysis on each of the five supports tested.

	Quantity of photons available for photocatalytic inactivation ($E\,s^{-1}$)
Ahlstrom	1.5×10^{-8}
P25 impregnated	1.6×10^{-8}
PC500 impregnated	1.8×10^{-8}
P25 suspended	1.7×10^{-8}
PC500 suspended	1.2×10^{-8}

Table 3
Photocatalytic inactivation efficiency on two growth media (DL: detection limit).

Supports	Time (min)	Photocatalytic inactivation efficiency (%)	
		TSA	EMB
Ahlstrom	20	7.12	17.16
	40	0.00	23.67
	60	0.00	52.34
	120	66.40	89.95
	140	98.85	99.73
	160	99.86	>99.99 (<DL)
PC500 impregnated	20	25.03	73.43
	40	46.32	79.24
	60	97.66	96.06
	120	99.54	99.47
P25 impregnated	20	81.23	96.55
	40	74.32	76.16
	60	85.47	92.81
	120	99.64	99.99
PC500 suspended	20	33.96	97.83
	40	84.17	99.76
	60	98.23	99.64
	120	99.89	>99.99 (<DL)
P25 suspended	20	99.09	99.92
	40	99.28	99.37
	60	99.82	99.99
	120	>99.99 (<DL)	>99.99 (<DL)

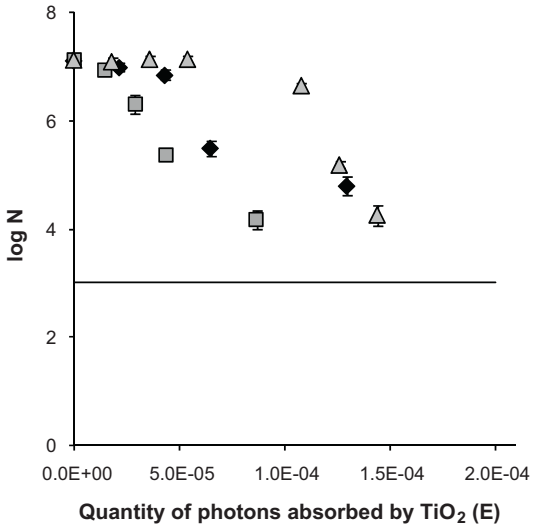

Fig. 6. How *E. coli* concentration evolves during photocatalysis on supports with TiO_2 PC500; growth medium: TSA (— detection limit, ▲ Ahlstrom, ■ PC500 suspended, ♦ PC500 impregnated).

3.3.2. Influence of photocatalytic support

The effect of the way in which TiO_2 is loaded onto supports (impregnated, with or without binder, or suspended) can be studied by comparing photocatalytic supports using the same TiO_2. *E. coli* inactivation for supports containing PC500 TiO_2 is shown in Fig. 6. For the same photon intensity, Ahlstrom is less effective than QMA impregnated with PC500, which in turn is less effective than PC500 in suspension, regardless of growth medium used to test viability.

The mass of TiO_2 varies depending on the support: 7.2 mg for Ahlstrom, 0.9 mg for QMA impregnated with PC500, 0.1 mg for suspended PC500 on QMA. These quantities are global and do not reflect the amount of TiO_2 actually in contact with biological particles, and thus available for their inactivation. On the Ahlstrom support, fibers are covered with a mixture of TiO_2, zeoliths and

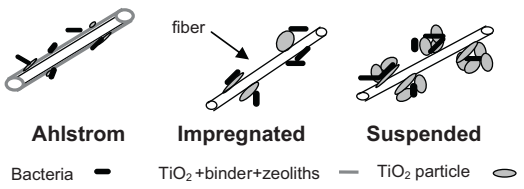

Fig. 7. Contact between TiO_2 and bacteria on the various supports.

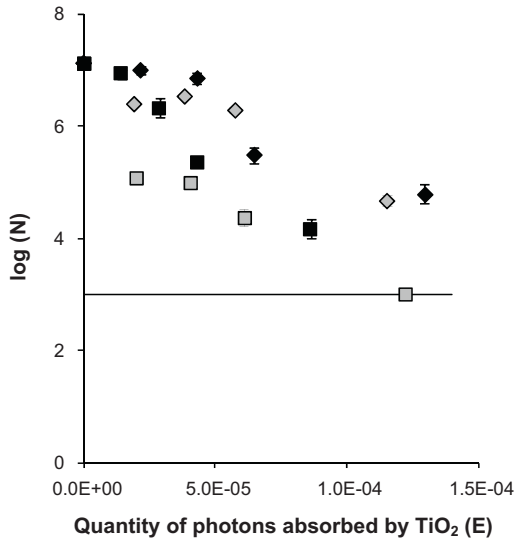

Fig. 8. Evolution of *E. coli* concentration during photocatalysis with two different TiO_2 qualities; growth medium: TSA (— detection limit, ■ PC500 suspended, ♦ PC500 impregnated, ■ P25 suspended, ◆ P25 impregnated).

inorganic binder. Thus, some titanium dioxide particles are masked on this support and will therefore be inaccessible to bacteria. For PC500-impregnated QMA, the mass of TiO_2 is lower than for Ahlstrom, but due to the absence of binder, the catalyst is more freely available for contact with bacteria. However, the way in which bacteria are distributed over fibers and TiO_2 is not controlled: bacteria can be attached on fiber without being in the vicinity of titanium dioxide. Finally, when bacteria are mixed with TiO_2 before being spread on the support, contact is optimized in comparison with the previous setups as bacteria can be trapped in TiO_2 nano-particle aggregates. These different situations are illustrated in Fig. 7. Efficient inactivation requires close contact between bacteria and titanium dioxide, as provided by the "suspended" condition.

3.3.3. *Effect of TiO_2 type*

Two TiO_2 types were tested: Millennium PC500 and Degussa P25. As indicated in Table 1, PC500 contains mainly anatase and P25 consists of 80% anatase, 20% rutile. PC500 also has a larger dispersed particle size than P25.

How the bacterial concentration changed as a function of the quantity of photons absorbed by TiO_2 for QMA filters with PC500 or P25, either suspended or impregnated, was studied (Fig. 8). For the same loading configuration, PC500 appears less efficient than P25, especially for the "suspended" configuration. This confirms recent observations by Lydakis-Simantiris et al. [39].

According to Nguyen et al. [40], dispersed particle sizes for TiO_2 PC500 are approximately three times larger than for TiO_2 P25. Thus, for the same mass of TiO_2, P25 provides a larger surface area for contact with bacteria than PC500. This may explain the improved efficiency. These observations highlight the fact that contact between TiO_2 and bacteria is key to photocatalytic efficiency.

Table 4
Experimental parameters determined for the Chick–Watson model.

	TSA		EMB	
	k'' ($min^{-1}\,g^{-1}$)	t_0 (min)	k'' ($min^{-1}\,g_{TiO_2}^{-1}$)	t_0 (min)
Ahlstrom	8.3	110	2.9	42
PC500 impregnated	25.7	13	22.0	0
P25 impregnated	17.4	0	26.9	0
PC500 suspended	274.5	8	509.1	0
P25 suspended	520.9	0	682.6	0

Another explanation of the increased activity of P25 could be that in this catalyst the electron/hole recombination is slower compared to other photocatalysts.

3.4. *Kinetic data*

Using equation 6, the inactivation constant (k'') and lag time (t_0) can be determined by plotting $1/m_{TiO_2}\ \log(N/N_0)$ versus t. For supports for which t_0 is less than or equal to zero, the lag time can be considered non-existent. In these cases, data were replotted according to the standard Chick-Watson model without lag time (Eq. (7)):

$$\frac{1}{m_{TiO_2}}\log\left(\frac{N}{N_0}\right) = -k''t \tag{7}$$

Results below the limit of detection were excluded. These calculations were performed for both growth media, results are presented in Table 4.

Thus, $k''_{\text{P25 suspended}} > k''_{\text{PC500 suspended}} > k''_{\text{P25 and PC500 impregnated}} > k''_{\text{Ahlstrom}}$. The same ranking order was obtained for the two growth media, and kinetic constants were of the same order of magnitude, indicating that kinetics are independent of growth conditions. In contrast, lag times plummet for analyses on EMB: for example for the Ahlstrom support, close to 2 h on TSA versus 40 min on EMB. Therefore, identifying the impact of photocatalysis and determining the parameters of the model depend on the growth medium chosen, as shown by the significant differences in lag times measured.

4. Conclusion

Photocatalytic degradation of bacterial cells consists of several (possibly interdependent) steps: bacterial inactivation (i.e. loss of viability), their degradation leading to release of cellular compounds, formation of by-products and progressive mineralization [41]. In the present work, inactivation of *E. coli* was studied on different photocatalytic supports. The experiments described showed that the quality of contact between bacteria and titanium dioxide must be optimized to improve degradation efficiency. Although photocatalytic mechanisms remain difficult to precisely understand, we have shown that photocatalysis induces metabolic damage to bacteria and that the kinetics of bacterial inactivation are well described by the classical Chick–Watson "black-box" model, including a lag time. To consider the overall process, we must now monitor photocatalytic mineralization of bacteria and identify its by-products. As *E. coli* is a Gram negative bacterium, its external membrane is composed of lipopolysaccharides or endotoxins. These components can induce headaches, fever or respiratory problems [42,43]. Thus, beyond its attractive bactericidal properties, photocatalysis should also eliminate endotoxins. Preliminary experiments confirm this assumption. However, analytical problems with the available endotoxins measurement method caused by the presence of support fibers in the analytical solution did not allowed a good assessment of their photocatalytic degradation.

Acknowledgments

The authors gratefully acknowledge Anaëlle Cloteaux for help with determining light flux by the Monte Carlo method.

References

[1] L. Fletcher, L. Gaunt, C. Beggs, S. Shepherd, P. Sleigh, C. Noakes, K. Kerr, Bactericidal action of positive and negative ions in air , BMC Microbiol. 7 (2007) 32–40.
[2] J. Noyce, J. Hughes, Bactericidal effects of negative and positive ions generated in nitrogen on *Escherichia coli* , J. Electrostat. 54 (2002) 179–187.
[3] K.P. Yu, G.W.M. Lee, S.Y. Lin, C.P. Huang, Removal of bioaerosols by the combination of a photocatalytic filter and negative air ions , J. Aerosol Sci. 39 (2008) 377–392.
[4] D.Y. Goswami, Decontamination of ventilation systems using photocatalytic air cleaning technology , J. Sol. Energy Eng. 125 (2003) 359–365.
[5] K.M. Lai, H.A. Burge, M.W. Firsy, Size and UV germicidal irradiation susceptibility of *Serratia Marcescens* when aerosolized from different suspending media , Appl. Environ. Microbiol. 70 (2004) 2021–2027.
[6] M. First, S.N. Ridnick, K.F. Banahan, R.L. Vincent, P.W. Brickner, Fundamental factors affecting upper-room ultraviolet germicidal irradiation: part I. Experimental , J. Occup. Environ. Hyg. 4 (2007) 321–331.
[7] G. Ko, M.W. First, H.A. Burge, The characterization of upper-room ultraviolet germicidal irradiation in inactivating airborne microorganisms , Environ. Health Perspect. 10 (2002) 95–101.
[8] J. Peccia, M. Hernandez, UV-induced inactivation rates for airborne *Mycobacterium bovis* BCG , J. Occup. Environ. Hyg. 1 (2004) 430–435.
[9] P.V. Scarpino, N.J. Jensen, P.A. Jensen, R. Ward, The use of ultraviolet germicidal irradiation (UVGI) in disinfection of airborne bacteria and rhinoviruses , J. Aerosol Sci. 29 (1998) 777–778.
[10] J.M. Herrmann, C. Guillard, Photocatalytic degradation of pesticides in agricultural used waters , C. R. Acad. Sci., Ser. IIc: Chim. 3 (2000) 417–422.
[11] N. Hamill, L. Weatherley, C. Hardacre, Use of a batch rotating photocatalytic contactor for the degradation of organic pollutants in wastewater , Appl. Catal., B 30 (2001) 49–60.
[12] S. Kim, S. Hong, Kinetic study for photocatalytic degradation of volatile organic compounds in air using thin film TiO_2 photocatalyst , Appl. Catal., B 35 (2002) 305–315.
[13] G. Zuo, Z. Cheng, H. Chen, G. Li, T. Miao, Study on photocatalytic degradation of several volatile organic compounds , J. Hazard. Mater. 128 (2006) 158–163.
[14] C. Guillard, T.H. Bui, C. Felix, V. Moules, B. Lina, P. Lejeune, Microbial disinfection of water and air by photocatalysis , C. R. Chimie 1 (2007) 107–113.
[15] C.Y. Lin, C.S. Li, Effectiveness of titanium dioxide photocatalyst filters for controlling bioaerosols , Aerosol Sci. Technol. 37 (2003) 162–170.
[16] S. Josset, J. Taranto, N. Keller, V. Keller, M.C. Lett, M.J. Ledoux, V. Bonnet, S. Rougeau, UV-A photocatalytic treatment of high flow rate air contamined with *Legionella pneumophila* , Catal. Today 129 (2007) 215–222.
[17] A. Pal, X. Min, L.E. Yu, S.O. Pehkonen, M.B. Ray, Photocatalytic inactivation of bioaerosols by TiO_2 coated membrane , Int. J. Chem. Reactor Eng. 3 (2005) 1–12.
[18] A.G. Rincon, C. Pulgarin, Photocatalytical inactivation of *E. coli*: effect of (continuous-intermittent) light intensity and of (suspended-fixed) TiO_2 concentration , Appl. Catal., B 44 (2003) 263–284.
[19] H.M. Coleman, C.P. Marquis, J.A. Scott, S.S. Chin, R. Amal, Bactericidal effects of titanium dioxide-based photocatalysts , Chem. Eng. J. 113 (2005) 55–63.
[20] A.G. Rincon, C. Pulgarin, Use of coaxial photocatalytic reactor (CAPHORE) in the TiO_2 photo-assisted treatment of mixed *E. coli* and *Bacillus* sp. and bacterial community present in wastewater , Catal. Today 101 (2005) 331–344.
[21] M. Cho, H. Chun, W. Choi, J. Yoon, Linear correlation between inactivation of *E. coli* and OH radical concentration in TiO_2 photocatalytic disinfection , Water Res. 38 (2004) 1069–1077.
[22] X. Simon, P. Duquenne, V. Koehler, C. Piernot, C. Coulais, M. Faure, Aerosolisation of *E. coli* and associated endotoxin using an improved bubbling bioaerosol generator , J. Aerosol Sci. 42 (2011) 517–531.
[23] D.S. Kim, S.Y. Kwak, Photocatalytic inactivation of *E. coli* with mesoporous TiO_2 coated film using the film adhesion method , Environ. Sci. Technol. 43 (2009) 148–151.
[24] A. Pal, S.O. Pehkonen, L.E. Yu, M.B. Ray, Photocatalytic inactivation of airborne bacteria in a continuous-flow reactor , Ind. Eng. Chem. Res. 47 (2008) 7580–7585.
[25] L. Caballero, K.A. Whitehead, N.S. Alle, J. Verran, Inactivation of *Escherichia coli* on immobilized TiO_2 using fluorescent light , J. Photochem. Photobiol. A 202 (2009) 92–98.
[26] A. Pal, S.O. Pehkonen, L.E. Yu, M.B. Ray, Photocatalytic inactivation of Gram-positive and Gram-negative bacteria using fluorescent light , J. Photochem. Photobiol. A 186 (2007) 335–341.
[27] J. Marugan, R. Van Grieken, C. Sordo, C. Cruz, Kinetics of the photocatalytic disinfection of *Escherichia coli* suspensions , Appl. Catal., B 82 (2008) 27–36.
[28] G. Spadoni, E. Bandini, F. Santarelli, Scattering effects in the photosensitized reactions , Chem. Eng. Sci. 33 (1978) 517–524.
[29] AFNOR. NF ISO 7218. Microbiologie des aliments-Règles générales pour les examens microbiologiques, 1996, 47.
[30] AFNOR, Analyse microbiologique-méthodes horizontales-Contrôle de la qualité des produits alimentaires , Recueil des normes françaises 1 (1996) 48–49.
[31] V.K. Pareek, A.A. Adesina, Light intensity distribution in a photocatalytic reactor using finite volume , AIChE J. 50 (2004) 1273–1288.
[32] G.E. Imoberdorf, F. Taghipour, M. Keshmiri, M. Mohseni, Predictive radiation field modeling for fluidized bed photocatalytic reactors , Chem. Eng. Sci. 63 (2008) 4228–4238.
[33] B. Ray, M.L. Speck, Freeze—injury in bacteria , Crit. Rev. Clin. Lab. Sci. 4 (1973) 161–213.
[34] S. Stewart, S. Grinshpun, K. Willeke, S. Terzieva, V. Ulevicius, J. Donnelly, Effect of impact stress on microbial recovery on an agar surface , Appl. Environ. Microbiol. 61 (1995) 1232–1239.
[35] F. Sayilkan, M. Asiltürk, N. Kiraz, E. Burunkaya, E. Arpaç, H. Sayilkan, Photocatalytic antibacterial performance of Sn^{4+}-doped TiO_2 thin films on glass substrate , J. Hazard. Mater. 162 (2009) 1309–1316.
[36] L. Liu, B. John, K. Yeung, Non-UV germicidal activity of fresh TiO_2 and Ag/TiO_2 , J. Environ. Sci. 21 (2009) 700–706.
[37] J.M.C. Robertson, P.K.J. Robertson, L.A. Lawton, A comparison of the effectiveness of TiO_2 photocatalysis and UVA photolysis for the destruction of three pathogenic micro-organisms , J. Photochem. Photobiol. A 175 (2005) 51–56.
[38] M. Cho, H. Chung, W. Choi, J. Yoon, Linear correlation between inactivation of *E. coli* and OH radicals concentration in TiO_2 photocatalytic disinfection , Water Res. 38 (2004) 1069–1077.
[39] N. Lydakis-Simantiris, D. Riga, E. Katsivela, D. Mantzavinos, N. Xekoukoulotakis, Disinfection of spring water and secondary treated municipal wastewater by TiO_2 photocatalysis , Desalination 1 (2010) 351–355.
[40] N. Nguyen, R. Amal, D. Beydoun, Photocatalytic reduction of selenium ions using different TiO_2 photocatalysts , Chem. Eng. Sci. 60 (2005) 5759–5769.
[41] Z. Huang, P.C. Maness, D.M. Blake, E.J. Wolfrum, S.L. Smolinski, W.A. Jacoby, Bactericidal mode of titanium dioxide photocatalysis , J. Photochem. Photobiol. A 130 (2000) 163–170.
[42] V. Liebers, M. Raulf-Heimsoth, T. Brüning, Health effects due to endotoxin inhalation (review) , Arch. Toxicol. 82 (2008) 203–210.
[43] V.H.-C. Liao, C.-P. Chio, W.-C. Chou, Y.-R. Ju, C.-M. Liao, Modeling human health risks of airborne endotoxin in homes during the winter and summer seasons , Sci. Total Environ. 408 (2010) 1530–1537.